Fundamental Bubbling Characteristics in a Rotating Fluidized Bed: Modeling and Measurement of bubble size

Hideya Nakamura, Tomohiro Iwasaki, Satoru Watano
Department of Chemical Engineering, Osaka Prefecture University,
Sakai, Osaka, Japan

Abstract

Modeling and measurement of bubble size in a rotating fluidized bed (RFB) were conducted. The model for predicting the bubble growth in RFB has been proposed based on the following concepts: (**i**) local centrifugal acceleration and excess gas velocity are considered as the parameters in the radial direction, and (**ii**) bubble volume flow locally changes depending on the radial distance. Bubbling behaviors were also experimentally observed by means of a high-sped video camera. Bubble sizes were measured using an image analysis technique, and the measured bubble sizes were compared with the estimated values by our proposed model and the available one for a conventional fluidized bed. The estimated bubble sizes by our proposed model showed good agreement with the measured ones, while the predicted ones by the model for conventional fluidized bed underestimated. The validity of our proposed concepts for modeling of bubble growth in RFB was confirmed.

1. Introduction

Fluidized bed has been used as gas-solid reactors and powder handling processors because of its high heat and mass transfer rates, temperature homogeneity, and favorable mixing property. Recently, a rotating fluidized bed (RFB) has attracted special interest due to its advantages: 1) it can prevent the growth of large bubbles at any high gas velocities by controlling the vessel rotational speed. It leads to improve the gas-solid contact and reaction efficiency, 2) it can fluidize very fine particles such as Geldart group C particles [1], since it imparts high centrifugal force and drag force to particles. From these advantages, RFB has been expected as some advanced industrial processes, such as reactor of rocket propulsion in a micro gravity field [2], the high efficiency dust filter [3], removal of NOx and soot from diesel engine exhaust gas [4], incineration of wool scouring sludges [5], granulation and coating of fine particles [6, 7] and handling of nano-particles [8, 9]. In spite of these previous studies, the reliable process has not been established yet, since the fundamental fluidization mechanisms are very complicated and have not been well studied yet. In order to conduct better design and control, it is very important to obtain a fundamental fluidization mechanism in RFB.

It has been well studied that bubbling characteristics in a gas-solid fluidized bed greatly influenced the fundamental fluidization phenomenon, such as gas-solid contact, particle mixing, entrainment, and so on. Therefore bubbling characteristics become critical parameters for design and control of fluidized bed. Nevertheless, the bubbling characteristic in RFB has not been reported anywhere. Only Chevray et al. [10] reported the mathematical model of bubble dynamics, such as velocity and trajectory, in RFB with vertical rotational axis. However, there was no experimental data for validity of their proposed model.

In this study, bubble size, which is one of the most important bubble characteristics, was analyzed in two-dimensional RFB. The mathematical model for predicting the bubble growth in RFB was proposed. The validity of the proposed model was evaluated by comparing the experimental bubble sizes measured by an image analysis with the estimated values by our proposed model and the available model for a conventional fluidized bed.

2. Rotating fluidized bed (RFB)

Figure 1 shows the schematic diagram of the rotating fluidized bed (RFB). The system consists of a cylindrical plenum chamber and a porous cylindrical air distributor rotating around its axis of symmetry inside the fixed plenum chamber. Due to the distributor rotational motion, particles are forced to move toward the rotating cylindrical air distributor, forming annular bed near at the air distributor. Air flows inward through the air distributor, and particles are balanced by drag and centrifugal forces, leading to achieve uniform fluidization in a high centrifugal force field.

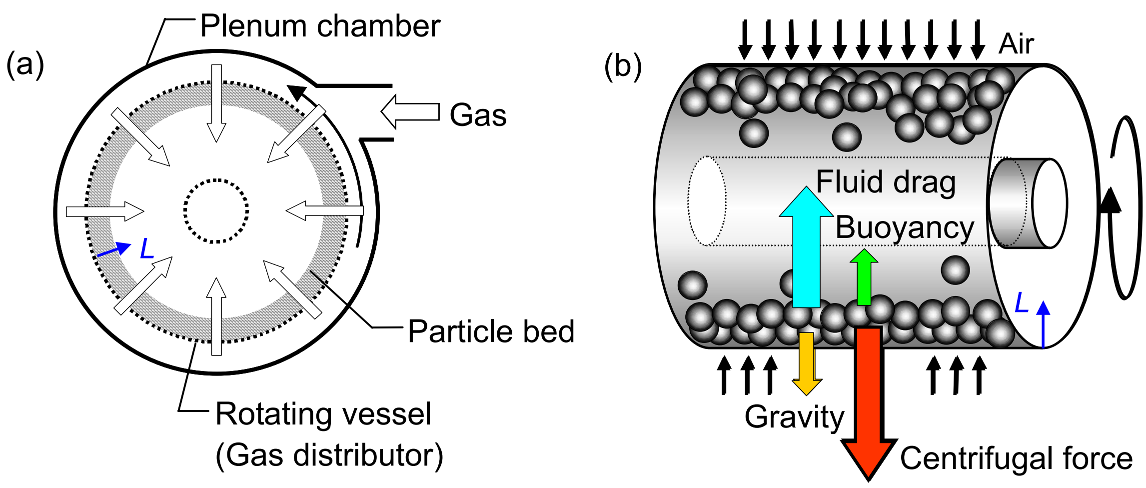

Figure 1. Rotating fluidized bed (RFB) system. (a) Front view; (b) side view.

3. Modeling of bubble growth in RFB

So far, many experimental and modeling studies have been reported for the prediction of the bubble growth in conventional fluidized bed. Darton et al. [11] has proposed a mathematical model of bubble growth for Geldart's Group B and D particles [1] based on the staged coalescence model assuming that bubble growth occurs in stage between adjacent two bubbles. According to this model, bubble diameter, D_b, can be expressed as follows [11]:

$$D_{\mathrm{b}} = \frac{0.54\left(u_0 - u_{\mathrm{mf}}\right)^{0.4}\left(L + 4.0\sqrt{A_{\mathrm{c}}}\right)^{0.8}}{g^{0.2}} \qquad (1)$$

where A_c is the area of distributor per orifice. However, available models for conventional fluidized bed cannot be directly applied to RFB, because the fluidization mechanisms are totally different. In this study, we modified the bubble growth model proposed by Darton et al. [11] based on the following new concepts for RFB: (**i**) the terms of acceleration and excess gas velocity are considered as a function of *L*, which is defined as a radial distance from rotating gas distributor as shown in Figure 1, and (**ii**) total mass flow of excess gas passing through the bed as bubbles increases with an increase in *L*.

According to Darton et al. [11], the bubble coalescence is assumed to occur in stages as shown in Figure 2.

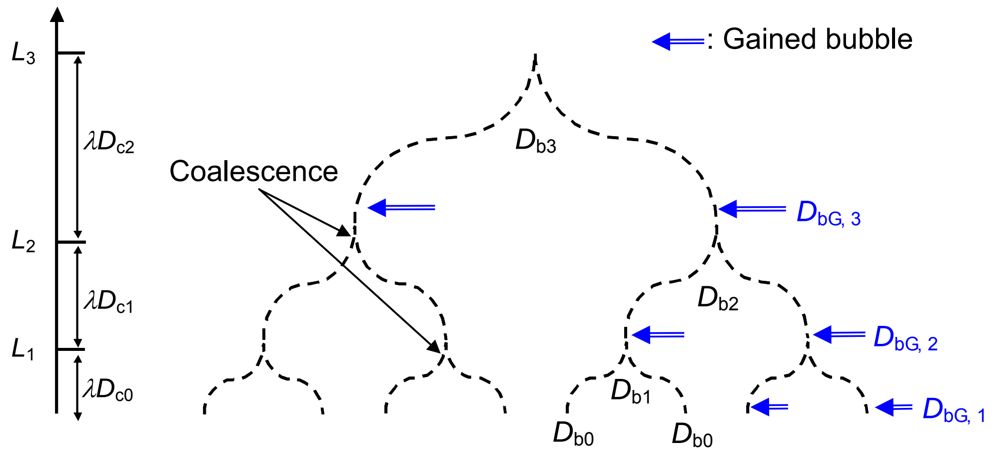

Figure 2. Schematic diagram of the proposed bubble growth model in RFB.

The distance L_N from the surface of the gas distributor at the *N* th stage of coalescence can be assumed as the following equation [11]:

$$L_N = \lambda D_{c0} + \lambda D_{c1} + \cdots + \lambda D_{c(N-1)} \quad (2)$$

where λ is a constant, which should be determined based on the experiment [11]. In this study, a value λ is set at 0.77 based on our experimental results. D_c also shows the equivalent diameter of the circle area of A_c ($A_c = 0.25\pi D_c^2$). Bubble diameter formed at perforated distributor can be also estimated by the following equation [12]:

$$D_b = 1.38 \left[\frac{u - u_{mf}}{g^{0.5}} A_c \right]^{0.4} . \quad (3)$$

Therefore, the correlation between the D_c and D_b at the *N* th stage of coalescence can be expressed as follows:

$$D_{cN} = 0.75 \frac{g'^{\,0.25}_N D_{bN}^{1.25}}{(u - u_{mf})_N^{0.5}} \quad (4)$$

where g'_N and $(u - u_{mf})_N$ show the local centrifugal acceleration and local excess gas velocity at L_N, respectively. These are expressed as follows [13]:

$$g'_N = \frac{G_0 g}{\beta_N} \tag{5}$$

$$\left(u - u_{\mathrm{mf}}\right)_N = \beta_N \cdot u_0 - \frac{1}{\beta_N}\frac{\mu}{\rho_{\mathrm{f}} d_{\mathrm{p}}}\left[\left(33.7^2 + 0.0408\frac{\rho_{\mathrm{f}}\left(\rho_{\mathrm{p}} - \rho_{\mathrm{f}}\right) d_{\mathrm{p}}{}^3 G_0 g}{\mu^2}\frac{1}{\beta_N}\right)^{0.5} - 33.7\right] \tag{6}$$

where G_0 is a dimensionless centrifugal factor, which is defined as a ratio of the centrifugal acceleration at the surface of rotating gas distributor to the gravitational acceleration ($g = 9.8$ m/s^2) as shown in the Eq. (7):

$$G_0 = \frac{R_{\mathrm{V}}\omega^2}{g} \tag{7}$$

where R_{V} and ω are radius and angular velocity of the rotating vessel. β in Eqs. (5) and (6) also indicates the dimensionless radius defined as:

$$\beta_N = \frac{R_{\mathrm{V}}}{\left(R_{\mathrm{V}} - L_N\right)} \quad . \tag{8}$$

The mass balance of the bubble volume in each coalescence stage can be expressed as follows:

$$\left.\begin{array}{l} D_{\mathrm{b}1}{}^3 = 2D_{\mathrm{b}0}{}^3 + 2D_{\mathrm{bG},1}{}^3 \\ D_{\mathrm{b}2}{}^3 = 2D_{\mathrm{b}1}{}^3 + 2D_{\mathrm{bG},2}{}^3 \\ D_{\mathrm{b}3}{}^3 = 2D_{\mathrm{b}2}{}^3 + 2D_{\mathrm{bG},3}{}^3 \\ \quad\vdots \qquad\quad \vdots \qquad\quad \vdots \\ D_{\mathrm{b}(N-1)}{}^3 = 2D_{\mathrm{b}(N-2)}{}^3 + 2D_{\mathrm{bG},(N\text{-}1)}{}^3 \end{array}\right\} \tag{9}$$

where, $D_{\mathrm{bG},\,N}$ shows the “gained bubble diameter” at N th coalescence stage due to an increase of bubble volume, since the excess gas velocity increases with an increase in L. It can be estimated as:

$$D_{\mathrm{bG},\,N} = 1.38\left[\frac{\left(u - u_{\mathrm{mf}}\right)_N - \left(u - u_{\mathrm{mf}}\right)_{(N-1)}}{g'_{(N-1)}{}^{0.5}} A_{\mathrm{c}(N-1)}\right]^{0.4} \tag{10}$$

In this study, the correlation between the bubble diameter and the dimensionless radius could be obtained by sequentially solving the above equations.

4. Experimental

Figure 3 shows the experimental set-up for visualization of bubbling behavior in the RFB. A thin porous cylindrical plate (I.D. 250 mm × D 5 mm), which was made of stainless sintered mesh with 20 μm openings, was used as rotating gas distributor. The front covers of the chamber and rotating vessel are both made of transparent acrylic plastic that allows observation of bubbling behavior at various circumferential locations. Spherical glass beads (FUJISTONE GB-01, Fuji-rika industrial Co., Ltd.) were used as experimental model particles and their median diameter and particle density was 136 μm and 2520 kg/m^3, respectively. The particles of 170.0 g were charged into the vessel of which the initial bed height was 31 mm.

The bubbling behavior in the two-dimensional RFB was observed by means of a high-speed video camera (FASTCAM MAX, Photoron Co., Ltd.). The recording frame rate and shutter speed were set at 3,000 to 4,000 frames/sec and 0.14 μs, respectively. A metal halide lamp was used as light source, which was set at backside of the particle bed.

Figure 4 shows the representative recorded images of the bubbling behaviors at various positions. The digitized recorded images consisted of 512×256 picture elements (pixel). The whole visualized area was 16 cm × 8 cm, which corresponded to 0.16 mm × 0.16 mm of spatial resolution per one pixel.

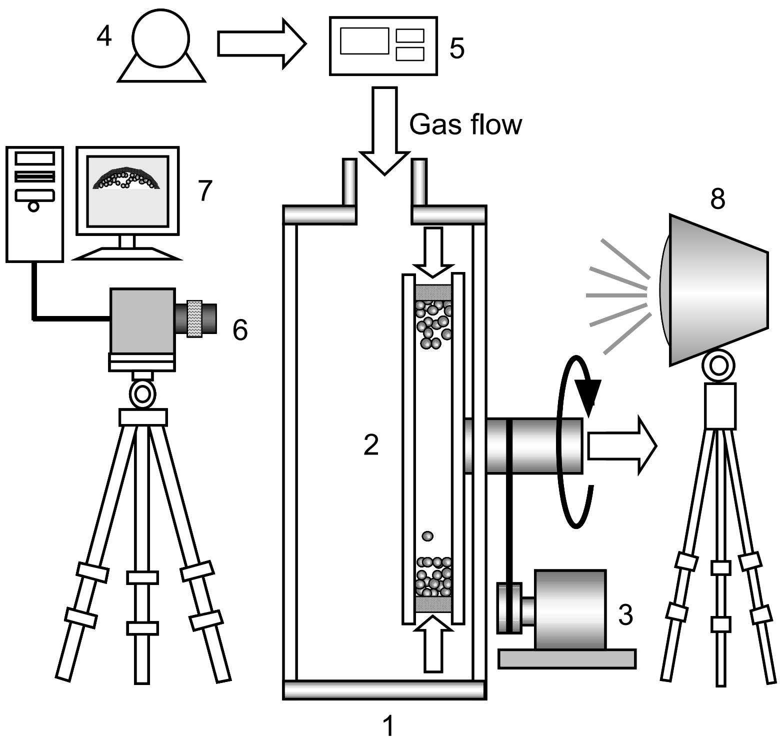

Figure 3. Experimental set up. (1) Plenum chamber; (2) rotating vessel (gas distributor; I.D. 250 mm×D. 5 mm); (3) motor; (4) blower; (5) mass flow meter; (6) high-speed video camera; (7) data acquisition system for high-speed video camera; (8) metal halide lamp.

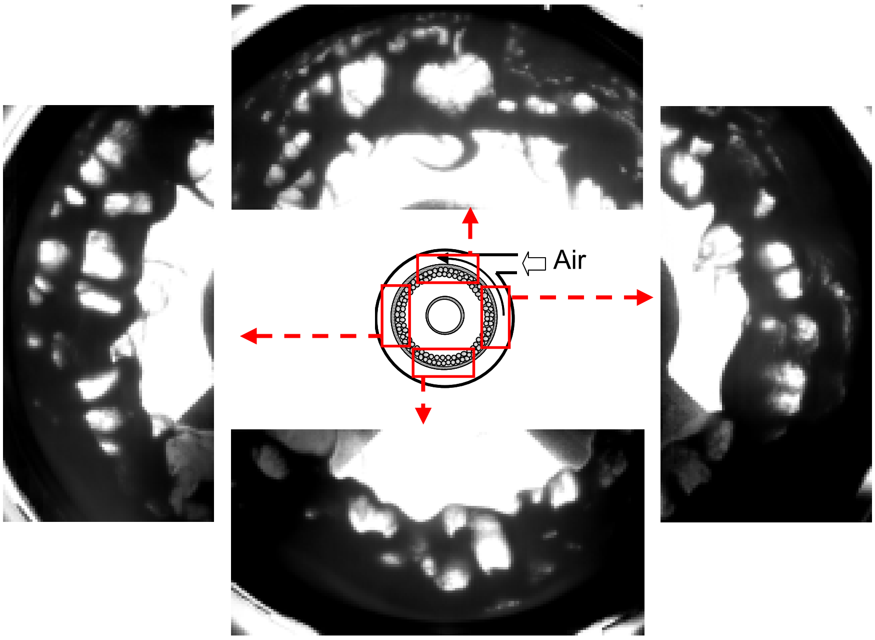

Figure 4. Visualized bubbling behavior in RFB. G_0=20.0; $(u–u_{mf})|_{L=0}$ =0.170 m/s.

Bubble sizes in the two-dimensional RFB were measured by an image analysis technique [14, 15]. Bubble diameter was individually obtained as an equivalent diameter of sphere by a following equation:

$$D_b = \left(\frac{6}{\pi} A_b H\right)^{1/3} \tag{11}$$

where A_b is the white projected area of individual bubble in the binarized image, and H is the bed thickness. The position of the bubble can also be calculated as the center of gravity of the white projected area. Finally, the volume averaged bubble diameter, $\overline{D_b}$, was calculated by a following equation:

$$\overline{D_b} = \left(\frac{6}{\pi} \overline{V_b}\right)^{1/3} \tag{12}$$

where $\overline{V_b}$, which is the averaged volume of bubble in the range of certain β~β+ $\Delta\beta$, was obtained by the following equation:

$$\overline{V_b} = \frac{\pi}{6} \int_0^\infty D_b{}^3 \phi(D_b) \mathrm{d}D_b \tag{13}$$

where $\phi(D_b)dD_b$ show the number fraction of bubble within the D_b~D_b+ dD_b.

The thresholding has a significant effect on the measured value in this technique. Therefore, the threshold value for binarization was precisely determined by a discriminant analysis method [16].

5. Results and discussion

Figure 5 shows the averaged bubble diameter in the RFB as a function of dimensionless radius, β. Dotted curve shows the predicted value by the model for conventional fluidized bed proposed by Darton et al. [11] expressed as the Eq. (1). Here, centrifugal acceleration at the surface of the gas distributor ($9.8 \cdot G_0$) was substituted for gravity term (g) in the Eq. (1). Solid curve is the predicted one by our proposed model.

Bubble diameters increased with an increase in β, and the predicted bubble diameter by our proposed model showed good agreement with the experimental ones, while the model proposed by Darton et al. [11] underestimated the experimental results. Figure 6 also shows comparison between experimental and estimated bubble diameters at various operating parameters. It is also clear that our proposed model can estimate bubble diameters with a higher accuracy than the model proposed by Darton et al. [11]. Here, some error can be observed in low bubble diameter: the experimental results showed larger values than the estimated ones. This is because that the small bubbles could not be visualized due to the limit of the depth of the vessel; the bubble, which was larger enough than the vessel depth, could only be observed. Therefore, it can be considered that the actual D_b in lower range become smaller than the experimental one in Figure 6.

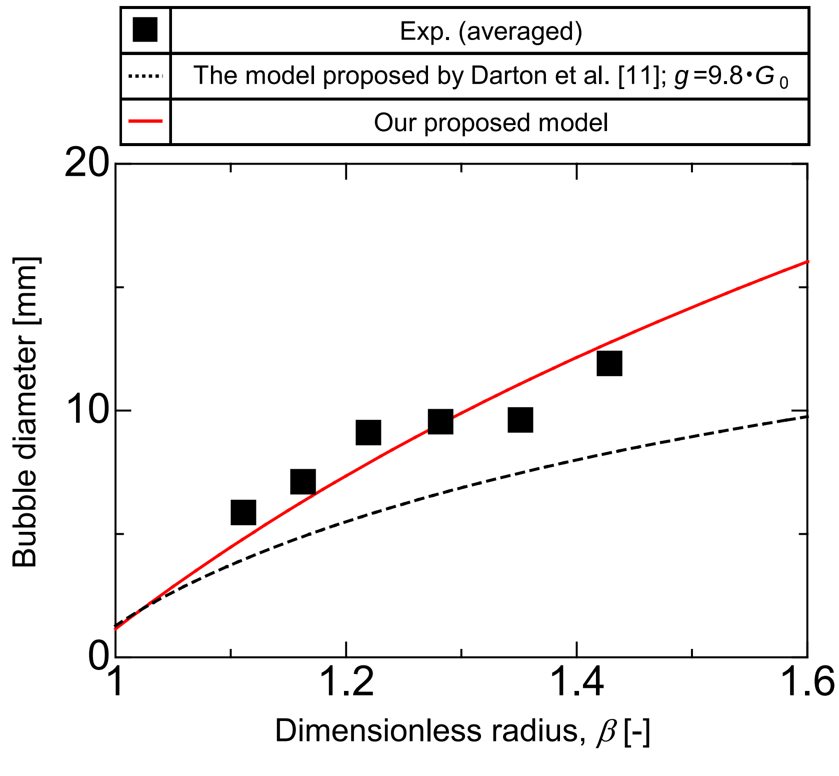

Figure 5. Bubble diameter as a function of dimensionless radius. G_0=10.0; $(u\text{-}u_{mf})_{L=0}$=0.170 m/s.

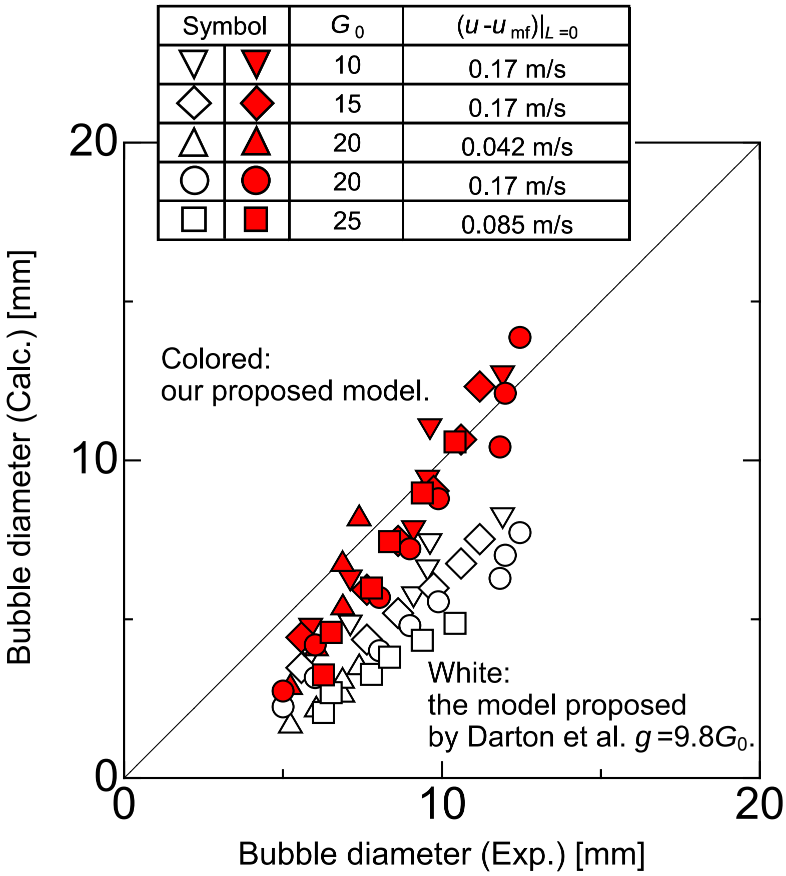

Figure 6. Comparison between experimental and estimated results of bubble diameters. Colored and white symbols indicate the estimated results by our proposed model and the model proposed by Darton et al. [11], respectively.

6. Conclusions

Modeling and measurement of bubble growth in the two-dimensional RFB were conducted. The estimated bubble size by our proposed model showed good agreement with the measured ones, while the predicted ones by the model for conventional fluidized bed proposed by Darton et al [11] underestimated the experimental results. The validity of our proposed concepts for modeling of bubble growth in RFB were thus completely confirmed: (**i**) the terms of acceleration and excess gas velocity are considered as a function of a radial distance from rotating gas distributor, and (**ii**) total mass flow rate of excess gas passing through the bed as bubbles increases with an increase in a radial distance from rotating gas distributor.

It can be expected that the mechanisms of other fluidization behaviors in RFB (e.g. heat and mass transfer, particle mixing, and so on) would be made clear based on our proposed model.

Acknowledgment

We acknowledge financial support by the Grant-in-Aids for JSPS Research Fellow from the Ministry of Education, Science, Sports and Culture of Japan.

Notation

A_b = area of white projected bubble image, m^2
A_c = area of distributor per orifice, m^2
D_c = equivalent diameter of circle area of A_c, m
D_b = equivalent spherical bubble diameter, m
D_{bG} = gained bubble diameter, m
d_p = particle diameter, m
G_0 = dimensionless centrifugal factor, nondimensional
g = gravitational acceleration = 9.8 m/s^2
g' = local centrifugal acceleration, m/s^2
H = bed thickness, m
L = radial distance from rotating gas distributor, m
R_V = radius of vessel, m
u = superficial gas velocity, m/s
u_0 = superficial gas velocity at gas inlet, m/s
u_{mf} = minimum fluidization velocity, m/s
$\overline{V_b}$ = averaged bubble volume, m^3

Greek letters

β = dimensionless radius, nondimensional
λ = constant in Eq. (2), nondimensional
μ = gas viscosity, Pa·s
ρ_f = gas density, kg/m^3
ρ_p = particle density, kg/m^3
ω = angular velocity of rotating vessel, rad/s

Subscript

N = sequential number of bubble coalescence

References

[1] Geldart D. Types of gas fluidization. *Powder Technol.* 1973;7:285-292.
[2] Ludewig H, Manning AJ, Raseman CJ. Feasibility of rotating fluidized bed reactor for rocket propulsion. *J. Spacecraft*. 1974; 11: 65-71.
[3] Pfeffer R, Tardos GI, Gal E. The use of a rotating fluidized bed as a high efficiency dust filter. Fluidization V. 1986;667-674.
[4] Tsutsumi A, Ju W, Yoshida K. Reduction of NO in diesel exhaust by soot using a centrifugal fluidized bed. *AIChE Symp. Ser*. 1996;92:86-90.
[5] Wong, WY, Lu, Y, Nasserzadeh VS, Swithenbank J, Shaw T, Madden M. Experimental investigation into the incineration of wool scouring sludges in a novel rotating fluidized bed. *J. Hazard. Mat*. 2000;B73:143-160.
[6] Watano S, Imada Y, Hamada K, Wakamatu Y, Tanabe Y, Dave RN, Pfeffer R. Microgranulation of fine powders by a novel rotating fluidized bed granulator. *Powder Technol*. 2003;131:250-255.

[7] Watano S, Nakamura H, Hamada K, Wakamatu Y, Tanabe Y, Dave RN, Pfeffer R. Fine particle coating by a novel rotating fluidized bed coater. *Powder Technol*. 2004;141:172-176.

[8] Matsuda S, Hatano H, Kuramoto K, Tsutsumi A, Fluidization of ultrafine particles with high G. *J. Chem. Eng. Japan*. 2001;34:121-125.

[9] Quevedo J, Pfeffer R, Shen Y, Dave R, Nakamura H, Warano S. Fluidization of nano agglomerates in a rotating fluidized bed. *AIChE J*. 2006;52:2401-2412.

[10] Chervray R, Chan YNI, Hill FB. Dynamics of bubbles and entrained particles in the rotating fluidized bed. *AIChE J*. 1980;26:390-398.

[11] Darton RC, Lanauze RD, Davidson JF, Harrison D. Bubble growth due to coalescence in fluidized bed. *Trans. IChemE.* 1977;55:274-280.

[12] Miwa T, Mori S, Kato T, Muchi I. Behavior of bubbles in gaseous fluidized bed. *Kagaku Kougaku*. 1971;35:770-776.

[13] Kao J, Pfeffer R, Tardos GI. On partial fluidization in a rotating fluidized bed. *AIChE J*. 1987;33:858-861.

[14] Lim KS, Agarwal PK, Oneill BK. Measurment and modeling of bubble parameters in a two-dimensional gas-fluidized bed using image analysis. *Powder Technol*. 1990;60:159-171.

[15] Shen L, Johnsson F, Leckner B. Digital image analysis of hydrodynamics two-dimensional bubbling fluidized beds. *Chem. Eng. Sci.* 2004;59:2607-2617.

[16] Tamura H. *Computational image processing* (in Japanese). Tokyo: Ohmsha;2002.